Table 1. Chemical mechanism for atmospheric mercury.

Reaction	Rate expression[a]	Reference[b]
Gas phase		
$Hg^0 + Br + M \rightarrow HgBr + M$	$1.46 \times 10^{-32}\ (T/298)^{-1.86}\ [Hg^0][Br][M]$	(1)
$HgBr + M \rightarrow Hg^0 + Br + M$	$1.6 \times 10^{-9}\ (T/298)^{-1.86} \exp(-7801/T)[HgBr][M]$	(2)
$HgBr + Br \rightarrow Hg^0 + Br_2$	$3.9 \times 10^{-11}\ [HgBr][Br]$	(3)
$HgBr + NO_2 \rightarrow Hg^0 + BrNO_2$	$3.4 \times 10^{-12} \exp(391/T)[HgBr][NO_2]$	(4)
$HgBr + Br \xrightarrow{M} HgBr_2$	$3.0 \times 10^{-11}\ [HgBr][Br]$	(3) [c]
$HgBr + NO_2 \xrightarrow{M} HgBrNO_2$	$k_{NO_2}([M], T)\ [HgBr][NO_2]$	(4) [d]
$HgBr + Y \xrightarrow{M} HgBrY$	$k_{HO_2}([M], T)\ [HgBr][Y]$	(4) [d, e]
$Hg^0 + Cl + M \rightarrow HgCl + M$	$2.2 \times 10^{-32} \exp(680(1/T - 1/298))[Hg^0][Cl][M]$	(5)
$HgCl + Cl \rightarrow Hg^0 + Cl_2$	$1.20 \times 10^{-11} \exp(-5942/T)[HgCl][Cl]$	(6) [f]
$HgCl + Br \xrightarrow{M} HgBrCl$	$3.0 \times 10^{-11}\ [HgCl][Br]$	(3) [c, g]
$HgCl + NO_2 \xrightarrow{M} HgClNO_2$	$k_{NO_2}([M], T)\ [HgCl][NO_2]$	(4) [d, g]
$HgCl + Y \xrightarrow{M} HgClY$	$k_{HO_2}([M], T)\ [HgCl][Y]$	(4) [d, e, g]
Aqueous phase [h]		
$Hg^0_{(aq)} + O_{3(aq)} \rightarrow Hg^{II}_{(aq)} +$ products	$4.7 \times 10^7\ [Hg^0_{(aq)}][O_{3(aq)}]$	(7)
$Hg^0_{(aq)} + HOCl_{(aq)} \rightarrow Hg^{II}_{(aq)} + OH^-_{(aq)} + Cl^-_{(aq)}$	$2 \times 10^6\ [Hg^0_{(aq)}][HOCl_{(aq)}]$	(8), (9) [i]
$Hg^0_{(aq)} + OH_{(aq)} \rightarrow Hg^{II}_{(aq)} +$ products	$2.0 \times 10^9\ [Hg^0_{(aq)}][OH_{(aq)}]$	(10), (11)
$Hg^{II}_{(aq)} + h\nu \rightarrow Hg^0_{(aq)}$	$\alpha j_{NO_2}\ [OA][Hg^{II}_{(aq)}]$	this work [j]

[a] Rate expressions for gas-phase reactions have units of molecule cm^{-3} s^{-1} where [ ] denotes concentration in number density units of molecules cm^{-3}, [M] is the number density of air, and T is temperature in K. Rate expressions for aqueous-phase reactions have units of M s^{-1} and $[\ ]_{(aq)}$ denotes concentration in M (mol L^{-1}). Henry's law coefficients (M atm^{-1}) relating gas-phase and aqueous-phase concentrations are $1.28 \times 10^{-1} \exp(2482(1/T - 1/298))$ for Hg^0 (Sanemasa, 1975), $1.1 \times 10^{-2} \exp(2400(1/T - 1/298))$ for O_3 (Jacob, 1986), $6.6 \times 10^2 \exp(5900(1/T - 1/298))$ for HOCl (Huthwelker et al., 1995), and 1.4×10^6 for Hg^{II} ($HgCl_2$; Lindqvist and Rodhe, 1985). The concentration of $OH_{(aq)}$ is estimated as given in the text. Lifetimes of Hg^I species are sufficiently short that steady-state can be assumed at all times.

[b] (1) Donohoue et al., 2006; (2) Dibble et al., 2012; (3) Balabanov et al., 2005; (4) Jiao and Dibble, 2017; (5) Donohoue et al. 2005; (6) Wilcox, 2009; (7) Munthe, 1992; (8) Lin and Pehkonen, 1998; (9) Wang and Pehkonen (2004); (10) Lin and Pehkonen, 1997; (11) Buxton et al., 1988.

[c] This is an effective rate constant for intermediate pressures most relevant for atmospheric oxidation and uses a higher level of theory than Goodsite et al. (2004).

[d] $k([M], T) = \left(\frac{k^0(T)[M]}{1 + k^0(T)[M]/k^\infty(T)}\right) 0.6^p$, where $p = \left(1 + \left(\log_{10}\left(k^0(T)[M]/k^\infty(T)\right)\right)^2\right)^{-1}$. Values of $k^0(T)$ and $k^\infty(T)$ are tabulated by Jiao and Dibble (2017) for different temperatures. At T = {220, 260, 280, 298, 320} K $k^0_{NO_2}$ = {27.4, 13.5, 9.52, 7.10, 5.09} $\times 10^{-29}$ cm^6 molecule^{-2} s^{-1}; $k^\infty_{NO_2}$ = {22.0, 14.2, 12.8, 11.8, 10.9} $\times 10^{-11}$ cm^3 molecule^{-1} s^{-1};

Hannah Horowitz 4/20/2017 2:12 PM
Deleted: Mechanism

Hannah Horowitz 4/20/2017 2:12 PM
Deleted: redox chemistry

Hannah Horowitz 4/20/2017 2:12 PM
Deleted: HgBr

Hannah Horowitz 4/20/2017 2:12 PM
Deleted: HgBr

Hannah Horowitz 4/20/2017 2:12 PM
Deleted: [

Hannah Horowitz 4/20/2017 2:12 PM
Deleted: for atmospheric purposes.

$k^{0}_{HO_2}$ = {8.40, 4.28, 3.01, 2.27, 1.64} × 10^{-29} cm^6 $molecule^{-2}$ s^{-1}; $k^{\infty}_{HO_2}$ = {14.8, 9.10, 7.55, 6.99, 6.11} × 10^{-11} cm^3 $molecule^{-1}$ s^{-1}.

[e] We assume that the rate coefficient determined for HgBr + HO_2 holds more generally for Y ≡ HO_2, OH, Cl, BrO, and ClO based on the similarity in their elementary reactions with HgBr and estimates from Wang et al. (2014).

[f] Abstraction alone competes with oxidation to Hg^{II} for HgCl as the rate of HgCl thermal dissociation is negligibly slow (Holmes et al., 2009).

[g] HgCl + Y rate coefficients are assumed to be the same as HgBr + Y. ClHg-Y and BrHg-Y have similar bond energies (Dibble et al., 2012).

[h] Oxidation of $Hg^{0}_{(aq)}$ takes place in clouds only, with concentrations of $Hg^{0}_{(aq)}$ and aqueous-phase oxidants determined by Henry's law equilibrium (footnote *a*). Aerosol liquid water contents under non-cloud conditions are too low for these reactions to be significant. Photoreduction of $Hg^{II}_{(aq)}$ takes place in both aqueous aerosols and clouds, with gas-aerosol partitioning of Hg^{II} as given by Amos et al. (2012) outside of clouds and Henry's law equilibrium for $HgCl_2$ in cloud (footnote *a*). The aerosol is assumed aqueous if RH > 35%.

[i] OCl^- has similar kinetics as HOCl but is negligible for typical cloud and aerosol pH given the HOCl/OCl^- pK_a = 7.53 (Harris, 2002).

[j] Parameterization for photoreduction of aqueous-phase Hg^{II}-organic complexes. Here j_{NO2} (s^{-1}) is the local photolysis rate constant for NO_2 intended to be representative of the near-UV actinic flux, [OA] (μg m^{-3} STP) is the mass concentration of organic aerosol under standard conditions of temperature and pressure (p = 1 atm, T = 273 K), and α = 5.2 × 10^{-2} m^3 STP $μg^{-1}$ is a coefficient adjusted in GEOS-Chem to match observed TGM concentrations (see text).

Hannah Horowitz 4/20/2017 2:12 PM
Deleted: similar binding energies (Goodsite et al., 2004; Dibble et al., 2012)

Hannah Horowitz 4/20/2017 2:12 PM
Deleted: *ab initio* calculations

Table 2. Reactions not included in chemical mechanism.[a]

Reaction	Reference[b]	Note
$Hg^0 + Br_2 \xrightarrow{M} HgBr_2$	Balabanov et al. (2005); Auzmendi-Murua et al. (2014)	*c*
$Hg^0 + Cl_2 \xrightarrow{M} HgCl_2$	Auzmendi-Murua et al. (2014)	*c*
$Hg^0 + I_2 \xrightarrow{M} HgI_2$	Auzmendi-Murua et al. (2014)	*c*
$Hg^0 + Br_2 \rightarrow HgBr + Br$	Auzmendi-Murua et al. (2014)	*d*
$Hg^0 + Cl_2 \rightarrow HgCl + Cl$	Auzmendi-Murua et al. (2014)	*d*
$Hg^0 + I_2 \rightarrow HgI + I$	Auzmendi-Murua et al. (2014)	*d*
$Hg^0 + OH \rightarrow HgO + H$	Hynes et al. (2009)	*d*
$Hg^0 + OH \xrightarrow{M} HgOH$	Goodsite et al. (2004); Hynes et al. (2009)	*e*
$HgOH + O_2 \rightarrow HgO + HO_2$	Shepler and Peterson (2003); Hynes et al. (2009)	*d*
$Hg^0 + HO_2 \xrightarrow{M} HgOOH$	Dibble et al. (2012)	*e*
$Hg^0 + NO_3 \xrightarrow{M} HgONO_2$	Dibble et al. (2012)	*e, f*
$Hg^0 + I \xrightarrow{M} HgI$	Greig et al. (1970); Goodsite et al. (2004); Subir et al. (2011)	*e, g*
$Hg^0 + BrO \xrightarrow{M} HgBrO$	Balabanov and Peterson (2003); Balabanov et al. (2005); Dibble et al. (2012, 2013)	*e, h*
$Hg^0 + ClO \xrightarrow{M} HgClO$	Balabanov and Peterson (2003); Dibble et al. (2012, 2013)	*e, h*
$Hg^0 + HCl \rightarrow Hg^{II} + \text{products}$	Hall and Bloom (1993); Subir et al. (2011)	*g*
$Hg^0 + O_3 \rightarrow Hg^{II} + \text{products}$	see note	*i*
$HgBr + I \xrightarrow{M} HgBrI$	see note	*j*
$HgBr + IO \xrightarrow{M} HgBrOI$	see note	*j*
$Hg^0_{(aq)} + HOBr_{(aq)} \rightarrow Hg^{II}_{(aq)} + OH^-_{(aq)} + Br^-_{(aq)}$	Wang and Pehkonen (2004); Hynes et al. (2009)	*k*
$Hg^0_{(aq)} + OBr^-_{(aq)} + H^+ \rightarrow Hg^{II}_{(aq)} + OH^- + Br^-_{(aq)}$	Wang and Pehkonen (2004); Hynes et al. (2009)	*k*
$Hg^0_{(aq)} + Br_{2(aq)} \rightarrow Hg^{II}_{(aq)} + 2Br^-_{(aq)}$	Wang and Pehkonen (2004); Hynes et al. (2009)	*k*
$Hg^{II}_{(aq)} \xrightarrow{HO_2/O_2^-} Hg^{I}_{(aq)} \xrightarrow{HO_2/O_2^-} Hg^0$	Gårdfeldt and Jonsson (2003)	*d*
$HgSO_{3(aq)} \rightarrow Hg^0_{(aq)} + \text{products}$	van Loon et al. (2001)	*l*

[a] These reactions have been reported in past literature but are now thought to be too slow to be of atmospheric relevance.
[b] References supporting non-inclusion in the chemical mechanism.
[c] Reaction reported in laboratory studies by Ariya et al. (2002), Yan et al. (2005, 2009), Liu et al. (2007), Raofie et al. (2008), and Qu et al. (2010), but not supported by theory.
[d] Endothermic reaction.
[e] The Hg^I compounds are weakly bound and thermally dissociate too fast to allow for 2nd step of oxidation to Hg^{II}.
[f] Peleg et al. (2015) find a strong correlation between observed nighttime gaseous Hg^{II} and NO_3 radical concentrations in Jerusalem. There is theoretical evidence against NO_3 initiation of Hg^0 oxidation (Dibble et al., 2012), and NO_3 may instead serve as the second-stage oxidant of Hg^I. This would be important only in warm urban environments where nighttime NO_3 is high.
[g] Found to be negligibly slow.
[h] The formation of compounds with structural formulae BrHgO and ClHgO requires a prohibitively high activation energy. Note *e* applies to compounds with structural formulae HgBrO, HgOBr, HgClO, and HgOCl.
[i] The direct formation of $HgO_{(s)}$ from this reaction is energetically unfavorable (Calvert and Lindberg, 2005; Tossell, 2006). It has been postulated that intermediate products like HgO_3 could lead to the formation of stable $(HgO)_n$ oligomers or $HgO_{(s)}$ via decomposition to $OHgOO_{(g)}$ (Subir et al., 2011), but these must be stabilized through heterogeneous reactions on atmospheric aerosols (Calvert and Lindberg, 2005) and the associated mechanism is unlikely to be significant in the atmosphere (Hynes et al., 2009). A gas-phase reaction has been reported in chamber studies (Hall, 1995; Pal and Ariya, 2004; Sumner et al., 2005; Snider et al., 2008; Rutter et al., 2012), but this is

Hannah Horowitz 4/20/2017 2:12 PM
Deleted: inferred from kinetic studies and/or included

Hannah Horowitz 4/20/2017 2:12 PM
Deleted: models

likely to have been influenced by the walls of the chamber (as seen in Pal and Ariya, 2004) and presence of secondary organic aerosols (in Rutter et al., 2012).
[j] Atmospheric concentrations of I and IO (Dix et al., 2013; Prados-Roman et al., 2015; Volkamer et al., 2015) are too low for these reactions to be significant.
[k] Rates are too slow to be of relevance.
[l] Concentrations of $HgSO_3$ under typical atmospheric SO_2 levels are expected to be very low.

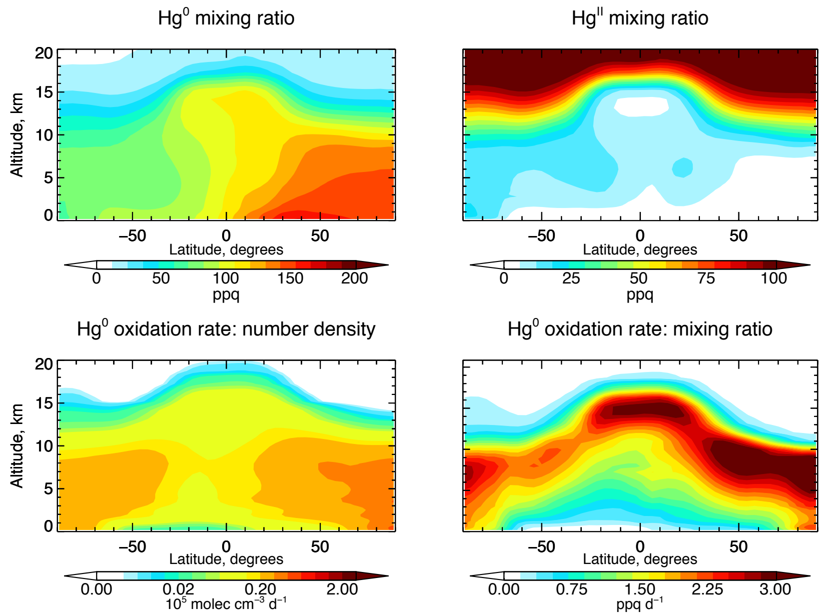

Figure 1. Annual (2009-2011) zonal mean mixing ratios of Hg^0 and Hg^{II} in GEOS-Chem, and Hg^0 oxidation rates in number density and mixing ratio units.

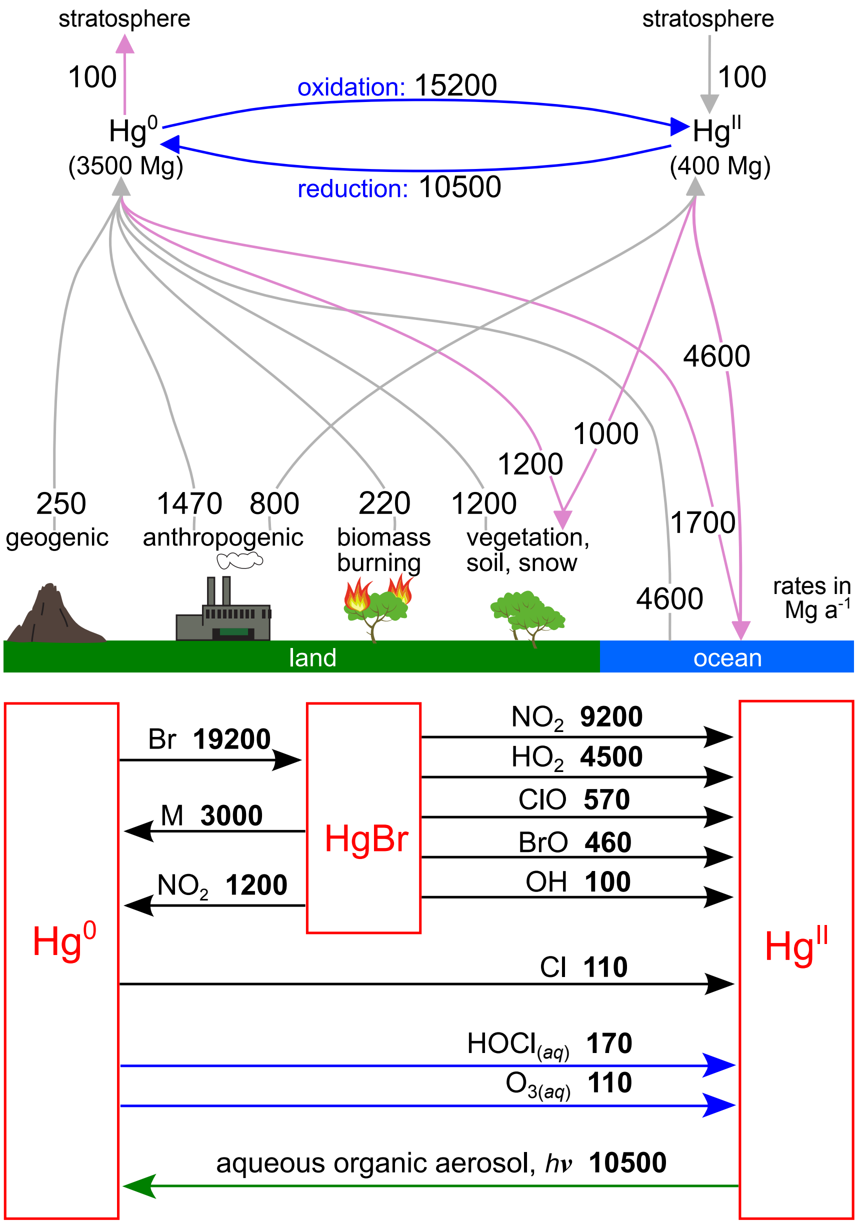

Figure 2. Global budget of tropospheric mercury in GEOS-Chem. Hg^{II} includes gaseous and particulate forms in local thermodynamic equilibrium (Amos et al., 2012). The bottom panel identifies the major chemical reactions from Table 1 cycling Hg^0 and Hg^{II}. Reactions with global rates lower than 100 Mg a^{-1} are not shown.

Hannah Horowitz 4/20/2017 2:12 PM

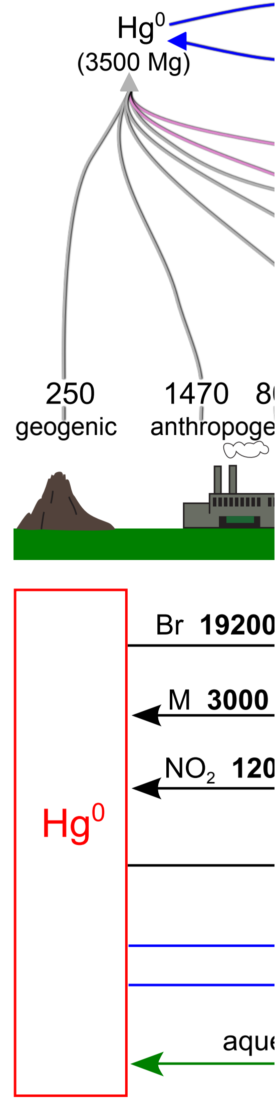

Deleted:

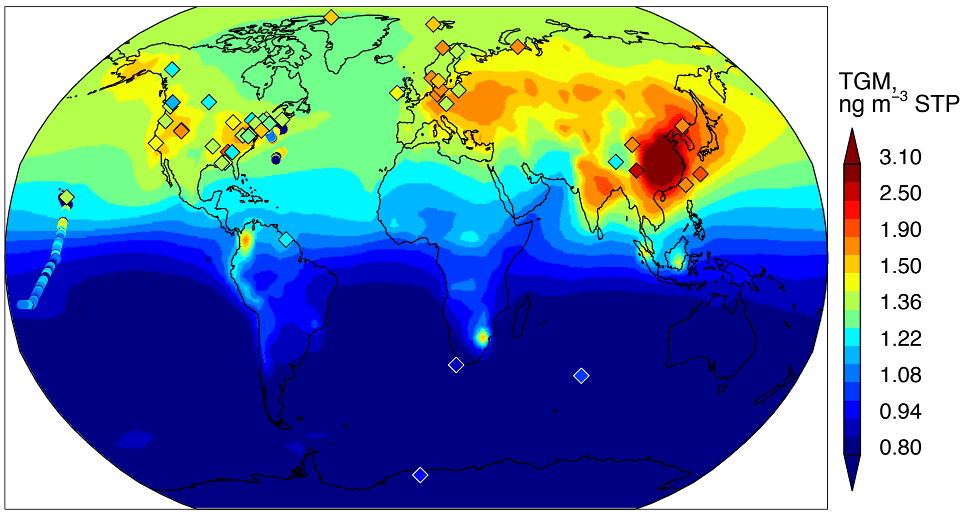

Figure 3. Global distribution of total gaseous mercury (TGM) concentrations in surface air in ng m^{-3} STP (p = 1 atm, T = 273 K). Model values (background) are annual means for 2009-2011. Observations (symbols) are for 2007-2013. Data for land sites (diamonds) are annual means for 2007-2013 as previously compiled by Song et al. (2015) and Zhang et al. (2016). Observations from 2007-2013 ship cruises (circles) are from Soerensen et al. (2013, 2014). Note the change in the linear color scale at 1.50 ng m^{-3}.

Hannah Horowitz 4/20/2017 2:12 PM

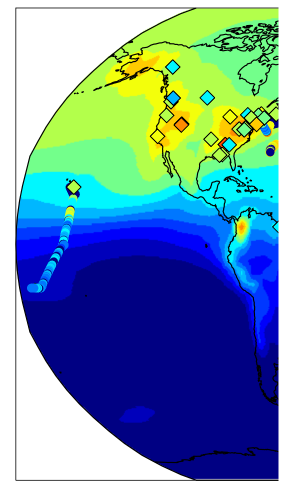

Deleted:

Hannah Horowitz 4/20/2017 2:12 PM

Deleted: .

Hannah Horowitz 4/20/2017 2:12 PM

Deleted: **Data at three Nordic stations were converted from 20°C to ng m^{-3} STP (p = 1 atm, T = 273 K) (see Slemr et al., 2015).**

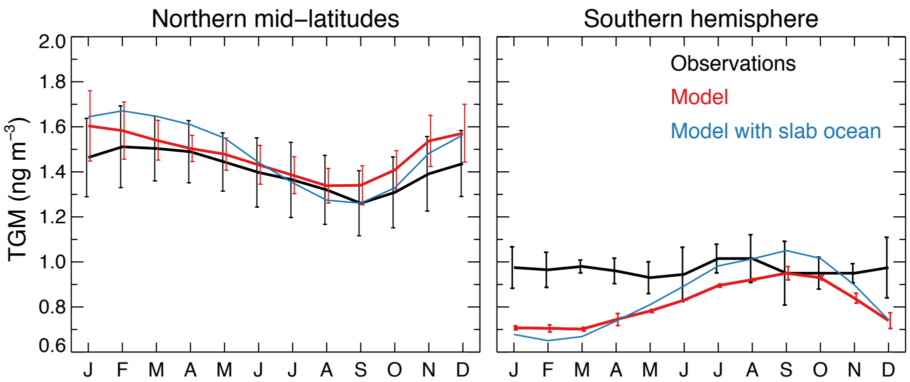

Figure 4. Mean seasonal variation and spatial standard deviation of total gaseous mercury (TGM) concentrations for northern mid-latitude sites (see Figure 3) and southern hemisphere sites (Amsterdam Island and Cape Point). Observations are compared to our standard GEOS-Chem simulation coupled to the MITgcm 3-D ocean model and to a sensitivity simulation coupled to the 2-D surface-slab ocean model in GEOS-Chem.

Hannah Horowitz 4/20/2017 2:12 PM
Deleted: results from

Hannah Horowitz 4/20/2017 2:12 PM
Deleted: (based on GEOS-Chem

Hannah Horowitz 4/20/2017 2:12 PM
Deleted:)

Hannah Horowitz 4/20/2017 2:12 PM
Deleted: study with

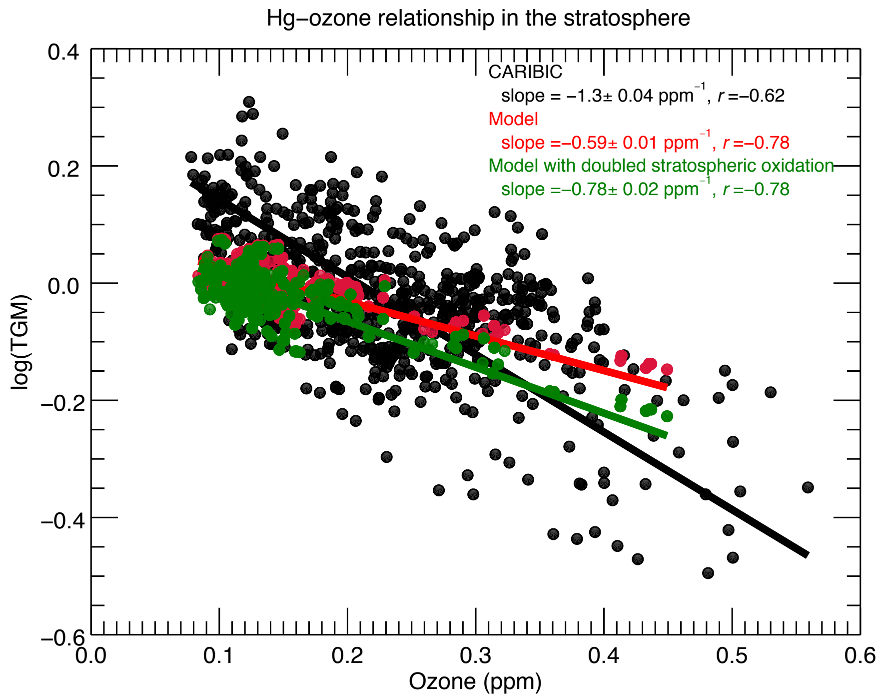

Figure 5. Relationship between total gaseous mercury (TGM) and ozone concentrations in the lower stratosphere. TGM is shown as the decimal logarithm of the concentration in ng m^{-3} STP. Observations are from CARIBIC commercial aircraft in the extratropical northern hemisphere for April 2014-January 2015 (Slemr et al., 2015). Tropospheric data as diagnosed by [O_3]/[CO] < 1.25 mol mol^{-1} are excluded. Model points are data for individual flights sampled along the CARIBIC flight tracks on the GEOS-Chem 4°x5° model grid. Also shown are results from a model sensitivity simulation with a doubled Hg^0 oxidation rate in the stratosphere. Reduced-major-axis (RMA) regressions for the log(TGM)-ozone relationship are shown with slopes and correlation coefficients *(r)*. Errors on the slopes are estimated by the bootstrap method.

Hannah Horowitz 4/20/2017 2:12 PM

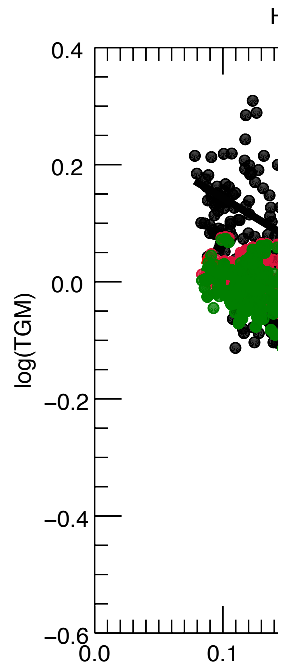

Deleted:

Hannah Horowitz 4/20/2017 2:12 PM

Deleted: .

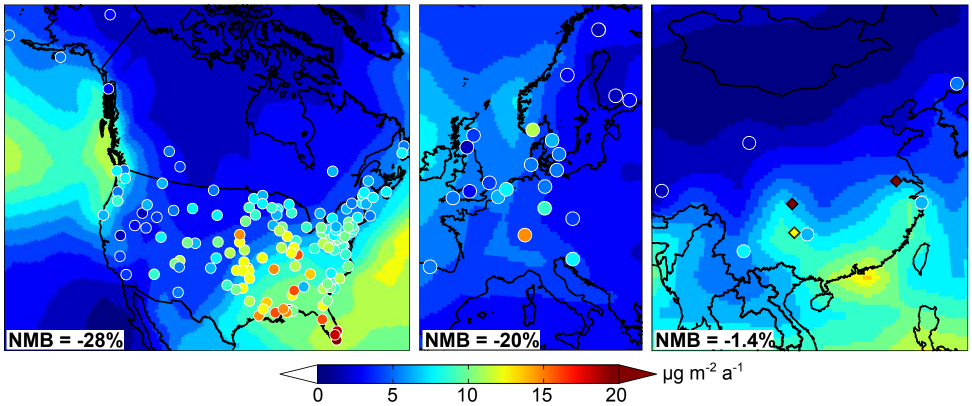

Figure 6. Annual Hg wet deposition fluxes over North America, Europe, and China. Model values for 2009-2011 (background contours) are compared to 2007-2013 observations from the Mercury Deposition Network (MDN, National Atmospheric Deposition Program, http://nadp.sws.uiuc.edu/mdn/) over North America (58 sites), the European Monitoring and Evaluation Program (EMEP) over Europe (20 sites), and data from Fu et al. (2015, 2016) over China (9 sites). In the China panel, circles represent rural sites and diamonds represent urban sites as identified in Fu et al. (2015, 2016). For the MDN and EMEP networks, which collect weekly or monthly integrated samples, we only include sites with at least 75% of annual data for at least one year between 2007 and 2013; for China we only include sites with at least 9 months of data over the 2007-2013 period. MDN data are formally quality-controlled, while for EMEP data we rely on a subset of sites that have been quality-controlled (Oleg Travnikov, personal communication). Legends give the normalized mean bias (NMB) for all sites, excluding urban sites in China.

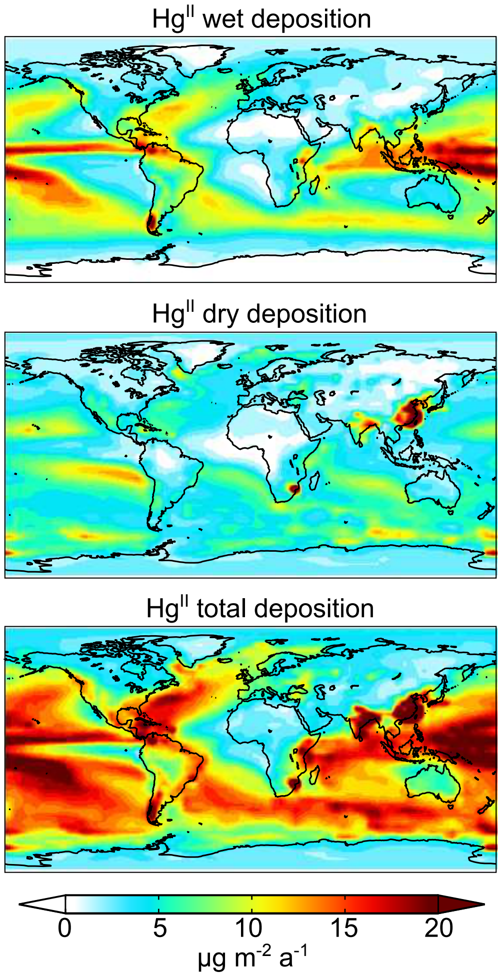

Figure 7. Annual 2009-2011 Hg^{II} deposition fluxes in GEOS-Chem.